increase in rate constant when alkyl ligands are replaced by aryl ligands is that donor–acceptor overlap is enhanced and thus κ is increased.

The interpretation of the rate variation can be tested by consideration of the activation parameters. If κ is increasing, then $\Delta S^\ddagger$ should increase toward zero and $\Delta H^\ddagger$ should be constant. The value of $\Delta S^\ddagger$ at 0.1 M salt is somewhat lower for the tolyl and anisyl isocyanide complexes than it is for the alkyl complexes. The value of $\Delta H^\ddagger$ varies for all of the reactions. There is thus some corroboration of the interpretation, but the interpretation of $\Delta S^\ddagger$ values is difficult, and the differences are small considering the precision of the measurements. Some of the complications in the interpretation of $\Delta S^\ddagger$ have been previously discussed for the manganese alkyl isocyanide complexes[4] and for ionic strength effects.[13]

In summary, we have found that electron self-exchange in the series of complexes $Mn(CNR)_6^{+/2+}$ is facilitated if the R group is aromatic and thus conjugated with the Mn—C≡N unit. The most likely reason for this rate enhancement is enhanced overlap between the donor and acceptor orbitals and thus an increase in the electronic transmission coefficient κ.

Acknowledgment. We thank Prof. John Hunt for helpful discussions and comments on the manuscript, Don Appel for assistance with the NMR measurements, the Boeing Co. for funds to purchase the Nicolet instrument, and the National Science Foundation for support.

Registry No. $Mn(CN\text{-}p\text{-}C_6H_4CH_3)_6^+$, 48243-20-5; $Mn(CN\text{-}p\text{-}C_6H_4CH_3)_6^{2+}$, 48243-19-2; $Mn(CN\text{-}p\text{-}C_6H_4OCH_3)_6^+$, 48244-70-8; $Mn(CN\text{-}p\text{-}C_6H_4OCH_3)_6^{2+}$, 52394-17-9.

Supplementary Material Available: Tables of reactant concentrations, temperatures, chemical shift values, and line widths (2 pages). Ordering information is given on any current masthead page.

---

(13) Brown, B. M.; Sutin, N. *J. Am. Chem. Soc.* **1979**, *101*, 883.

Contribution from the Departments of Chemistry, Tulane University, New Orleans, Louisiana 70118, and Colorado State University, Fort Collins, Colorado 80523

Formation and Photophysical Properties of Tetranuclear Bipyridyl Complexes of the Type $\{[(bpy)_2Ru(L\text{-}L)]_3Fe\}$

R. H. Schmehl,*[†] R. A. Auerbach,[†] W. F. Wacholtz,[†] C. M. Elliott,*[‡] R. A. Freitag,[‡§] and J. W. Merkert[‡]

Received November 4, 1985

The synthesis of a series of covalently linked bipyridines, L–L, having alkyl linkages ranging from $(CH_2)_2$ to $(CH_2)_{12}$ is described. The ligands are used to prepare a series of ruthenium complexes of the type $[(bpy)_2Ru(L\text{–}L)]^{2+}$. These complexes may be used as ligands in the formation of tetranuclear complexes having a central Fe^{2+}, $\{[(bpy)_2Ru(L\text{–}L)]_3Fe\}^{8+}$. The equilibrium constants for formation of the complexes as a function of the length of the alkyl bridge between the bipyridines are determined by spectrophotometric and fluorescence quenching methods. The emission decay of the ruthenium complexes in solutions containing Fe^{2+} is a double exponential. The fast component of the decay corresponds to emission from ruthenium "ligands" complexed to iron, and the long component of the decay is from uncomplexed ruthenium centers. The rapid decay of the complexed ruthenium results from energy transfer to the iron bipyridyl center of the complex.

Introduction

With the increasing interest in interfacial photoprocesses and the photochemistry of large aggregated chromophores,[1] there is a growing need to prepare and spectroscopically characterize small clusters of chromophores that may serve as models for larger, more complex systems. A significant body of literature exists describing supersensitization of semiconductors[1b,2] and intermolecular quenching and excimer formation processes of chromophores adsorbed to numerous colloids.[1a,3] Among the various chromophores used in these studies, derivatives of $[Ru(bpy)_3]^{2+}$ have been widely applied.[2d,4-9] Recently, covalently linked 2,2′-bipyridine derivatives (**1**–**4**) have been synthesized[10] (vide infra) that allow for the preparation of particular polynuclear bipyridine-containing complexes that are soluble in a variety of solvents. In this work we report the in situ complexation of $[(bpy)_2Ru(L\text{–}L)]^{2+}$ complexes (**1a**–**4a**) with iron(II) to form the tetranuclear complexes $\{[(bpy)_2Ru(L\text{–}L)]_3Fe\}^{8+}$ (**1b**–**4b**).

Excitation-energy transfer from coordinated ruthenium centers to the central iron bipyridyl complex occurs for each of the four complexes. The intramolecular energy transfer is analogous to that observed in organic donor–acceptor complexes linked by an alkyl chain[11] and represents a rare example of intramolecular energy transfer in an inorganic system having no ground-state electronic interaction between the donor and acceptor.

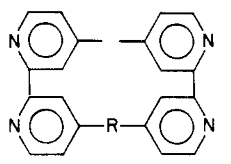

L-L

1, R = $(CH_2)_2$
2, R = $(CH_2)_5$
3, R = $p\text{-}(CH_2)_2(C_6H_4)(CH_2)_2$
4, R = $(CH_2)_{12}$

[†] Tulane University.
[‡] Colorado State University.
[§] Present address: Department of Chemistry, Davidson College, Davidson, NC 28036.

(1) See, for example: (a) Thomas, J. K. *The Chemistry of Excitation at Interfaces*; ACS Monograph 181; American Chemical Society: Washington, DC, 1984. (b) Grätzel, M., ed. *Energy Resources through Photochemistry and Catalysis*; Academic: New York, 1983.

(2) (a) Gerischer, H.; Willig, F. *Top. Curr. Chem.* **1976**, *61*, 31. (b) Honda, K.; Fujishima, A.; Watanabe, T. *Surface Electrochemistry*; Takamora, T.; Kozawa, A., Eds.; Japan Science Society: Tokyo, 1978; p 141. (c) Armstrong, N. R.; Mezza, T.; Linkous, C. L.; Thacker, B.; Klofta, T.; Cieslinski, R. *Chemically Modified Surfaces in Catalysis and Electrocatalysis*; Miller, J. S., Ed.; ACS Symposium Series 192; American Chemical Society: Washington, DC, 1982; Chapter 12. (d) Ghosh, P. K.; Spiro, T. *J. Am. Chem. Soc.* **1980**, *102*, 5543. (e) Giraudeau, A.; Fan, F.-R. F.; Bard, A. J. *J. Am. Chem. Soc.* **1980**, *102*, 5137. (f) Leempoel, P.; Fan, F.-R. F.; Bard, A. J. *J. Phys. Chem.* **1983**, *87*, 2948. (g) Kamat, P. V.; Fox, M. A. *J. Am. Chem. Soc.* **1984**, *106*, 119. (h) Faulkner, L. R.; Fan, F.-R.; Fischer, S. G. *Adv. Chem. Ser.* **1980**, *No. 184*, 113. (i) Nakao, M.; Watanabe, T.; Itoh, K.; Fujishima, A.; Honda, K. *Ber. Bunsenges. Phys. Chem.* **1984**, *88*, 17.

Table I. Equilibrium Constants for Formation of Complexes **1b**–**4b** in 1:1 Methanol:Water at 25 °C

complex	K_{eq}, M^{-3}	ε(525 nm),[a] M^{-1} cm^{-1}	$\phi_{complex}$	no. of determinations[c]
1b	(3.9 ± 3) × 10^{13}	7070 ± 500	0.005 ± 0.002	6
2b	(4.1 ± 0.5) × 10^{14}	6740 ± 500	0.017 ± 0.005	5
3b	(1.3 ± 0.5) × 10^{15}	7450 ± 500	0.016 ± 0.005	5
4b	(6.2 ± 4) × 10^{15}	6610 ± 500	0.015 ± 0.005	2
$[Fe(dmb)_3]^{2+}$ [b]	(3.1 ± 2) × 10^{17}	8420 ± 500		1

[a] Molar absorptivity of the tris(bipyridyl)iron portion of complexes **1b**–**4b** obtained from fits of ΔA(525 nm) vs. $[Fe]_T$. [b] dmb = 4,4′-dimethyl-2,2′-bipyridine. [c] total number of independent analyses from absorption and emission spectra.

Experimental Section

1,2-Bis(4′-methyl-2,2′-bipyridyl-4-yl)ethane (1). This ligand was prepared as described elsewhere.[10b]

1,5-Bis(4′-methyl-2,2′-bipyridyl-4-yl)pentane (2). Diisopropylamine (4.0 mL) (Aldrich) was added to 15 mL of dry THF (distilled from Na/benzophenone) under N_2 in a 0.5-L three-necked flask, and the solution was cooled to −78 °C. Next, 1.1 equiv of *n*-butyllithium (~1.0 M in hexane solution, Aldrich) was added via syringe and the solution stirred for 15 min. A 5.0-g (0.027-mol) sample of 4,4′-dimethyl-2,2′-bipyridine (Reiley Tar and Chemical, Indianapolis, IN), which had been previously recrystallized from ethyl acetate, was dissolved in ~150 mL of dry THF. This solution was added dropwise over 5 min to the cooled LDA solution described above. After the mixture was stirred for 2 h at −78 °C, 13.81 mL of 1,3-dibromopropane (1.0 equiv) was introduced quickly into the reaction mixture with vigorous stirring. The reaction was then allowed to warm to room temperature (over ~60 min) after which the reaction was quenched by the addition of 100 mL of H_2O. The entire reaction mixture was extracted three times with 100-mL portions of CH_2Cl_2, and all of the organic fractions were combined and rotary evaporated to dryness, leaving the crude product as a brown oil.

The oil was dissolved in a minimum amount of CH_2Cl_2, chromatographed on 60/200-mesh silica gel, and eluted with 10% (v/v) acetone in CH_2Cl_2. The desired ligand eluted as a colorless band, which was collected and rotary evaporated to dryness. The resulting oil solidified upon standing for 24 h at room temperature. The solid was finally recrystallized from ethyl acetate, yielding a white crystalline product. The resulting purified product was verified by 220-MHz NMR. The final yield of purified product was 3–4 g (57–76%).

1,12-Bis(4′-methyl-2,2′-bipyridyl-4-yl)dodecane (4). Ligand **4** was prepared in manner analogous to that of **2** except that 1,10-dibromodecane was employed. The product was chromatographed using 2% (v/v) acetone in CH_2Cl_2 as the eluent. Typical yields were 50%.

1,4-Bis[2-(4′-methyl-2,2′-bipyridyl-4-yl)ethyl]benzene (3). The ligand is prepared in the same way ligands **1**, **2**, and **4** are prepared up to the point of quenching the reaction. The reaction is quenched by adding one-half of the volume of the total reaction mixture of water. The precipitate formed is collected by filtration and washed with water (3 × 20 mL). The filtrate and combined washings are extracted with diethyl ether (3 × 100 mL). The ether fractions are collected, dried with anhydrous $MgSO_4$, filtered, and evaporated to dryness. The collected solids were mixed and recrystallized from ethanol. The crystalline solid showed a single spot by TLC on silica ($CHCl_3$). Anal. Calcd for the monohydrate $C_{32}H_{32}N_2O$ C, 78.68; H, 6.60; N, 11.46. Found: C, 79.91; H, 6.44; N, 11.325.

Preparation of $Ru(bpy)_2(L–L)^{2+}$ (L–L = 1, 2, 4) Ions 1a, 2a, and 4a. Complexes **1a**, **2a**, and **4a** were all prepared in identical fashion except for the dimer ligand employed. $Ru(bpy)_2Cl_2$, 0.10 g, was dispersed in ~50 mL of ethylene glycol and the solution brought briefly to reflux. The temperature was then reduced to 120 °C and a 30-fold excess of the appropriate dimer ligand (i.e. **1**, **2**, or **4**) was added. The reaction was stirred with heating for ~2 h. Over this time period the solution changed in color from a deep red-orange to a bright yellow-orange. The reaction mixture was cooled to room temperature, and the volume was increased to ~50 mL by the addition of distilled water. At this point the majority of the excess ligand precipitated. The solution was filtered and extracted twice with benzene. A concentrated solution of NH_4BF_4 was added to the water/ethylene glycol solution with stirring until the precipitation of $[Ru(bpy)_2(L–L)]^{2+}(BF_4^-)_2$ was complete, at which point the solution was nearly colorless. The product was filtered on a medium-porosity frit with suction and rinsed with a small portion (~1 mL) of cold H_2O. The solid was dried under vacuum at 45 °C for ~45 min, redissolved in a minimum of CH_2Cl_2, and filtered to remove excess NH_4BF_4. The final product was brought out of solution as the monohydrate by the rapid addition of 3–4 volumes of Et_2O to the CH_2Cl_2. The resulting $[Ru(bpy)_2(L–L)]^{2+}(BF_4^-)_2 \cdot H_2O$, was filtered, washed with ~25 mL of Et_2O, and dried under vacuum at 45 °C for ~10 min. Typical yields were 75%. Anal. Calcd for $RuC_{44}H_{38}N_8B_2F_8 \cdot H_2O$ (**1a**$(BF_4)_2$): C, 54.40; H, 4.15; N, 11.53. Found: C, 54.06; H, 3.99; N, 11.54. Calcd for $RuC_{47}H_{44}N_8B_2F_8 \cdot H_2O$ (**2a**$(BF_4)_2$): C, 55.69; H, 4.58; N, 11.05. Found: C, 55.78; H, 4.43; N, 10.45. Calcd for $RuC_{54}H_{58}N_8B_2F_8 \cdot H_2O$ (**4a**$(BF_4)_2$): C, 58.34; H, 5.44; N, 10.07. Found: C, 58.02; H, 5.25; N, 9.46.

Preparation of the $Ru(bpy)_2(L–L)^{2+}$ (L–L = 3) Ion 3a. A solution of **3** (466 mg, 9.90 × 10^{-4} mol) in 50 mL of ethanol was brought to reflux. To the colorless solution was slowly added a solution of $[Ru(bpy)_2Cl_2]$ (240 mg, 4.96 × 10^{-4} mol) in 10 mL ethanol dropwise. Upon complete addition (approximately 30 min), the solution was refluxed for 2 h. The reaction mixture was evaporated to dryness and dissolved in distilled water, and the excess ligand was removed by filtration. Saturated aqueous $NaBF_4$ was added dropwise, precipitating the product complex as an orange powder. The filtered, dried powder was chromatographed on neutral alumina with 1:1 acetonitrile:toluene eluent. Two orange bands exhibiting red luminescence eluted; the first band was taken to be **3a**$(BF_4)_2$. The monomeric complex, **3a**$(BF_4)_2$ was demonstrated to be free of the dinuclear impurity $[(bpy)_2Ru(L–L)Ru(bpy)_2]^{4+}$ by thin-layer chromatography on Alumina G (Analtech) plates using 1:1 CH_3CN:toluene (for **3a**, R_f 0.6; for the dinuclear complex, R_f 0.4). The product was reprecipitated from acetonitrile by dropwise addition to a large excess of ether. Yield after chromatography: 512 mg, 84%. Anal. Calcd for $C_{50}H_{42}N_8B_2F_8Ru \cdot 3H_2O$: C, 55.42; H, 4.46; N, 10.33. Found: C, 54.66; H, 4.28; N, 9.49.

Apparatus. All UV–vis absorption spectra were recorded on an HP 8451 single-beam diode-array spectrophotometer. Emission spectra were obtained by using a Spex Model 111C photon-counting fluorometer equipped with a 450-W Xe arc lamp (Osram), a cooled PMT housing, and a thermostated cell holder (maintained at 25 °C in all experiments). Luminescence lifetime measurements were made by using nitrogen laser excitation and right-angle detection of light emitted at 620 nm using a Hammamatsu R777 PMT monitored with a PAR 162 boxcar averager with a Model 166 gated integrator as described elsewhere.[12]

---

(3) (a) Thomas, J. K. *Acc. Chem. Res.* **1977**, *10*, 133. (b) Atik, S. S.; Thomas, J. K. *J. Am. Chem. Soc.* **1981**, *103*, 3550. (c) Moebius, D. *Acc. Chem. Res.* **1981**, *14*, 63. (d) Whitten, D. G.; Russell, J. C.; Schmehl, R. H. *Tetrahedron, Report No. 131* **1982**, *38*(16), 2455. (e) Meyerstein, D.; Rabani, J.; Matheson, M. S.; Meisel, D. *J. Phys. Chem.* **1978**, *82*, 1879. (f) Infelta, P. P.; Grätzel, M.; Thomas, J. K. *J. Phys. Chem.* **1974**, *78*, 190. (g) Fendler, J. H. *Acc. Chem. Res.* **1980**, *13*, 7. (h) Rothenberger, G.; Infelta, P. P.; Grätzel, M. *J. Phys. Chem.* **1981**, *85*, 1850.

(4) Kurimura, Y.; Nagashima, M.; Takato, K.; Tuchida, E.; Kareka, M.; Yamada, A. *J. Phys. Chem.* **1982**, *86*, 2432.

(5) (a) Ghosh, P. K.; Bard, A. J. *J. Phys. Chem.* **1984**, *88*, 5519. (b) Ghosh, P. K.; Mau, A. W.-H.; Bard, A. J. *J. Electroanal. Chem. Interfacial Electrochem.* **1984**, *169*, 315.

(6) (a) Baxendale, J. H.; Rodgers, M. A. J. *J. Phys. Chem.* **1982**, *86*, 4906. (b) Rodgers, M. A. J.; Wheeler, M. F. da Silva. *Chem. Phys. Lett.* **1978**, *53*, 16. (c) Schmehl, R. H.; Whitesell, L. G.; Whitten, D. G. *J. Am. Chem. Soc.* **1981**, *103*, 3761. (d) Dressick, W. J.; Havenstein, B. L., Jr.; Gilbert, T. B.; Demas, J. N.; DeGraff, B. A. *J. Phys. Chem.* **1984**, *88*, 3379. (e) Brugger, P. A.; Grätzel, M. *J. Am. Chem. Soc.* **1980**, *102*, 246.

(7) Duong Long, D.; Serpone, N.; Grätzel, M. *Helv. Chim. Acta* **1984**, *67*, 1012.

(8) Wolfgang, S.; Gafney, H. D. *J. Phys. Chem.* **1983**, *87*, 5395.

(9) Habti, A.; Keravis, D.; Levitz, P.; van Damme, H. *J. Chem. Soc., Faraday Trans. 2* **1984**, *80*, 67.

(10) (a) Elliott, C. M.; Freitag, R. A. *J. Chem. Soc. Chem. Commun.* **1985**, 156. (b) Elliott, C. M.; Freitag, R. A.; Blaney, D. D. *J. Am. Chem. Soc.* **1985**, *107*, 4647–4655.

(11) DeSchryver, F.; Boens, N. *Adv. Photochem.* **1977**, *10*, 359.

(12) Wacholtz, W. F.; Auerbach, R. A.; Schmehl, R. H. *Inorg. Chem.* **1986**, *25*, 227.

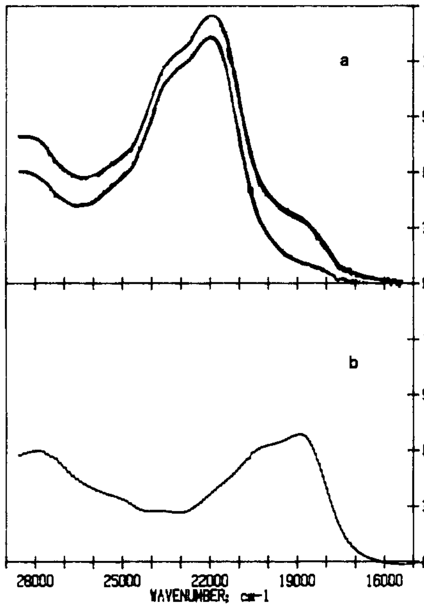

Figure 1. (a) Absorption spectra of complex **3a** (5×10^{-5} M) in 1:1 $CH_3OH:H_2O$ showing the increase in absorbance at 19 000 cm^{-1} upon addition of Fe(II). (b) Spectrum of complex **3a** (5×10^{-5} M) in the presence of 5×10^{-4} M Fe(II) after subtraction of the absorbance due to **3a**.

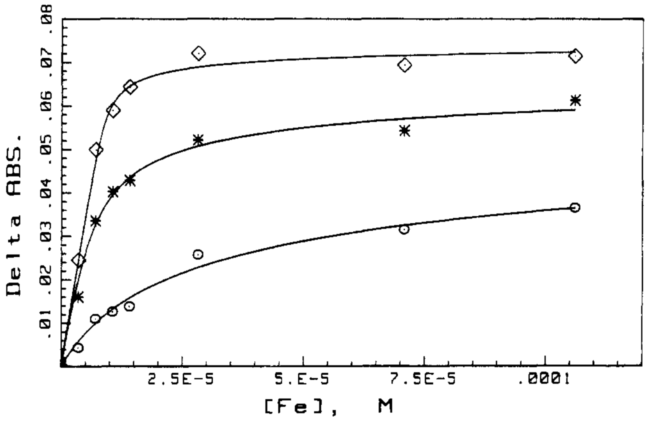

Figure 2. Increase in absorbance at 525 nm observed as a function of [Fe(II)] for 5×10^{-5} M solutions of **4a** (◇), **2a** (☆), and **1a** (○). Solid lines are best fits obtained for the data (see text).

Association of 1–4 with Fe(II). The in situ preparation and characterization of **1b–4b** was performed in 1:1 methanol:water (v/v) buffered to 0.1 M, pH 4 with sodium acetate/acetic acid and containing 1 mM hydroxylamine hydrochloride to prevent oxidation of the Fe(II). In a typical experiment, 2 mL of a solution containing the ruthenium complex ligand (20–200 μM) were mixed with 20–200 μL of a stock ferrous ammonium sulfate solution (1 mM) and diluted to 4 mL with buffer. The solutions were stored in the dark at 25 °C for 12 h, after which the absorption and emission spectra were recorded. Luminescence lifetime measurements were obtained on separate samples prepared in the same manner.

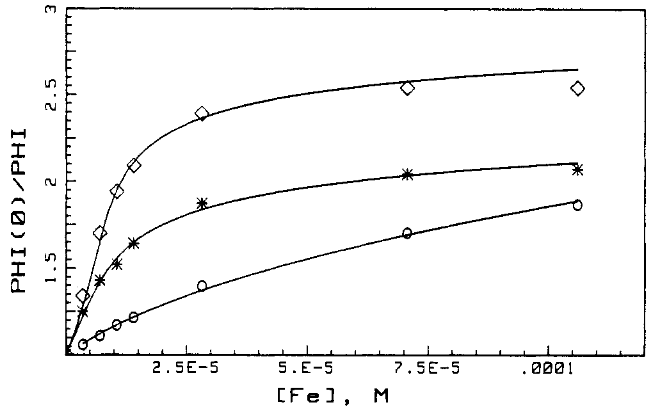

Figure 3. Relative emission intensity at 620 nm as a function of [Fe(II)] for 5×10^{-5} M solutions of **1a** (○), **2a** (☆), and **4a** (◇). The solid lines are determined from best fits of the data (see Experimental Section).

The peak molar absorptivity, ε, of the iron charge-transfer absorption of the complexes and the complex association equilibrium constants, K_a, can be determined by fitting the absorbance values of the difference spectra (Figure 2) as a function of total Fe^{2+} added at constant ruthenium concentration. A modified Marquadt algorithm was used for least-squares minimizations.[27] Fits were obtained to the function $\Delta A = \epsilon c$ where c, the concentration of **1b–4b** is calculated without approximation by means of Newton's iterative numerical method via the association equilibrium constant, total ruthenium concentration, and total iron concentration. Results of the fits are shown in Table I and Figure 2.

In a similar manner observation of the relative solution quantum yields for emission from **1a–4a** and **1b–4b** as a function of the total iron concentration at constant total ruthenium concentration ($[Ru]_T$) can be used to obtain K_a and the ratio of quantum yields of ruthenium emission for the complex ($\phi_{complex}$) to free ruthenium (ϕ_{free}). Given that the ruthenium charge-transfer absorption and emission is not spectroscopically changed by complexation (i.e., only the emission quantum yield is changed) then the ratio of emission intensities in the presence (I) and absence (I°) of iron is given by

$$I/I^\circ = 1 - (3c/[Ru]_T)(1 - \phi_{complex}/\phi_{free})$$

where c is the concentration of **1b–4b**. Fits to this function, given in Figure 3 and Table I, yield values of K_a in good agreement with absorption fits. Values of $\phi_{complex}/\phi_{free}$ are much higher than predicted based upon lifetime information (vide infra).

Results

Complex Stoichiometry. The spectrophotometric characteristics, redox behavior, emission spectra, and lifetimes **1a–4a** are very similar to those of the parent complex, $[Ru(bpy)_2(Me_2bpy)]^{2+}$.[12] Titration of **1a–4a** with Fe^{2+} in acetate-buffered solutions of 1:1 methanol:water results in spectrophotometric changes, shown in Figure 1, indicative of the Fe(II) → bpy metal-to-ligand charge transfer. The difference spectra for the absorption of **1a–4a** before and after the addition of Fe(II) are identical with the spectrum of $[Fe^{II}(Me_2bpy)_3]$. The stoichiometry of the Fe(II) complex with **1a–4a** was established by Job's method, where the absorbance due to the iron complex was determined as a function of the mole fraction of Fe(II). The mole fraction of Fe(II) having the largest

---

(13) Konig, E. *Coord. Chem. Rev.* **1968**, *3*, 471.

(14) Van Houten, J.; Watts, R. *J. Am. Chem. Soc.* **1976**, *98*, 4853.

(15) (a) Palmer, R. A.; Piper, T. S. *Inorg. Chem.* **1966**, *5*, 864. (b) Sutin, N.; Creutz, C. *Adv. Chem. Ser.* **1978**, *No. 168*, 1.

(16) (a) Quenching of $[Ru(bpy)_3]^{2+}$ by Fe(II) in 1:1 MeOH:water buffered to pH 4 occurs with a quenching rate constant of less than 1.1×10^7 M^{-1} s^{-1}. Solutions saturated in $Fe^{II}(NH_4)_2(SO_4)_2$ (approximately 0.02 M) exhibit I°/I values less than 1.1 for quenching of $[Ru(bpy)_3]^{2+}$. (b) Creutz, C.; Sutin, N. *Inorg. Chem.* **1976**, *15*, 496. (c) Laurence, G. S.; Balzani, V. *Inorg. Chem.* **1974**, *13*, 2976.

(17) Creutz, C.; Chou, M.; Netzel, T. L.; Okumura, M.; Sutin, N. *J. Am. Chem. Soc.* **1980**, *102*, 7309.

(18) Wacholtz, W. F., Tulane University, unpublished results.

(19) (a) See: Birks, T. B. *Photophysics of Aromatic Molecules*; Wiley-Interscience: London, 1970; pp 567–599. (b) Förster, T. H. *Discuss. Faraday Soc.* **1959**, *27*, 7.

(20) Dexter, D. L. *J. Chem. Phys.* **1953**, 21, 836.

(21) Bock, C. R.; Connor, J. A.; Gutierrez, A. R.; Meyer, T. J.; Whitten, D. G.; Sullivan, B. P.; Nagle, J. K. *J. Am. Chem. Soc.* **1979**, *101*, 4815.

(22) Fuoss, R. M. *J. Am. Chem. Soc.* **1972**, *94*, 75.

(23) Debye, P. *Trans. Electrochem. Soc.* **1942**, *82*, 265.

(24) (a: Schwarz, F. P.; Gouterman, M.; Maijiani, Z.; Dolphin, D. H. *Bioinorg. Chem.* **1972**, *2*, 1. (b) Lamola, A. A. *J. Am. Chem. Soc.* **1969**, *91*, 4786. (c) Keller, R. A. *J. Am. Chem. Soc.* **1968**, *90*, 1940.

(25) Cherry, W. R., unpublished results.

(26) Since the decay of excited states of **1b–4b** may be written $k^{obsd} = k_r + k_n + k_{EN}$, where $k_r + k_n$ are the radiative and nonradiative decay rates of **1a–4a** and k_{EN} is the intramolecular energy transfer rate, $k_{EN} = k^{obsd} - (k_r + k_n)$. It is assumed here that k_r and k_n are the same for both free **1a–4a** and the corresponding iron complexes.

(27) (a) Marquardt, D. W. *J. Soc. Ind. Appl. Math.* **1963**, *11*, 431. (b) Bevington, P. R. *Data Reduction and Error Analysis for the Physical Sciences*; McGraw-Hill: New York, 1969; pp 235–236.

Table II. Emission Spectral Characteristics of **1a–4a**

complex	λ_{max}(298 K), cm^{-1}	τ(298 K), ns	ϕ_{em}(298 K)[a]	τ(77 K), ns
1a	16 400	356 ± 8	0.052	4560 ± 20
2a	16 400	390 ± 10	0.048	4090 ± 17
3a	16 300	389 ± 10	0.048	4020 ± 17
4a	16 400	360 ± 10	0.048	4070 ± 33

[a] All quantum yields measured relative to $[Ru(bpy)_3]^{2+}$ in aqueous solution. Yields are ±0.005.

change in absorbance at 510 nm was 0.24 ± 0.02, indicating a complex stoichiometry of 3:1 **1a–4a**:Fe(II).

Isolation of the iron complex **3b** in pure form for characterization was attempted by precipitation of the tetranuclear complex with NH_4PF_6. Cyclic voltammetry of the precipitated complex in CH_3CN (supporting electrolyte, tetraethylammonium perchlorate; reference = SSCE) exhibits two reversible waves at +1.20 and +0.90 V, indicative of the Ru(III/II) and Fe(III/II) couples, respectively, for the tris(bipyridyl) complexes. The Ru:Fe ratio of the areas of the voltammetric waves was 4:1; TLC on alumina plates (CH_3CN/toluene eluent) shows two bands corresponding to free ruthenium complex **3a** and the tetranuclear iron containing complex **3b**. Preparative chromatographic separation on alumina of the tetranuclear complex from unreacted ruthenium was unsuccessful since decomposition of the tetranuclear complex occurs during chromatography. As a result the complex was prepared in situ from mixtures of the ruthenium complexes **1a–4a** (as BF_4^- salts) with ferrous ammonium sulfate in 1:1 methanol:water buffered to pH 4 (0.1 M acetate) and containing 5 mM hydroxylamine hydrochloride to prevent oxidation of iron(II) species in solution.

Complex Formation Equilibria. Spectrophotometric titrations of solutions having a fixed concentration of **1a–4a** (between 30 and 100 μM) with ferrous ion result in absorbance changes at 525 nm as shown in Figure 2 after the 12-h equilibration period. Equilibrium constants for association of Fe(II) with **1a–4a** to form the tetranuclear complexes **1b–4b** were determined from the growth in absorbance at 525 nm. It is assumed that the dinuclear and trinuclear iron complexes are not present in appreciable concentrations (see Experimental Section). For tris(bipyridyl)iron(II), the formation constant for complexation of the third bipyridine is much greater than the first two bipyridine association constants (K_1 = 16 000 M^{-1}; K_2 = 5000 M^{-1}; K_3 = 8 × 10^7 M^{-1}).[13] Table I lists equilibrium constants for association as well as molar extinction coefficients at 525 nm for the iron(II) bipyridyl portion of the tetranuclear complexes. The association constant for formation of $[Fe(Me_2bpy)_3]^{2+}$ under these conditions is a factor of 50 greater than that for **4b**. Analogous iron(II) bipyridyl complexes are formed for each case (**1b–4b**), and the molar absorptivities at 525 nm agree within the margins of error.

Quenching of the ruthenium bipyridyl emission occurs upon addition of Fe(II). Figure 3 shows that quenching of the emission does not follow Stern–Volmer kinetics and that the order of relative quenching is **4** > **3** $\simeq$ **2** > **1**. In fact the quenching mirrors absorption changes. Equilibrium constants from emission data were determined by assuming that dynamic quenching in the presence of Fe(II) does not occur ($k_q \leq 10^7$ M^{-1} s^{-1})[16] and that the observed emission in the presence of Fe(II) results only from free monomer (**1a–4a**) and the tetranuclear complex (**1b–4b**) as expressed in eq 1, where α is the fraction of total ruthenium

$$\phi_{em} = (1 - \alpha)(\phi^{\circ}_{free}) + \alpha(\phi_{complex}) \qquad (1)$$

complex associated with a tetranuclear cluster and ϕ°_{free} and $\phi_{complex}$ are the emission yields for the monomeric and tetranuclear complexes, respectively. Equilibrium constants obtained from α values were included in determination of K_{eq} values listed in Table I. Curves obtained from best fits of α and $\phi_{complex}/\phi_{free}$ are represented in Figure 3 (see Experimental Section), and $\phi_{complex}$ values are included in Table I.

Luminescence Lifetimes. In the absence of Fe(II) the emission of **1a–4a** at room temperature and 77 K is cleanly a single exponential. Table II lists luminescence lifetimes for the charge-transfer emission at 298 and 77 K and room-temperature-emission quantum yields relative to $[Ru(bpy)_3]^{2+}$ in aqueous solution[14] for complexes **1a–4a**. The lifetime and quantum yield for each complex is within 10% of the average for the four complexes, as expected given the similarity of the systems. In the presence of Fe(II) at concentrations equal to or greater than the ruthenium complex concentration (0.1–0.5 mM), a second very rapidly decaying component to the emission emerges. Figure 4 shows a typical emission decay for the mixed system on a 200-ns time scale. Emission spectra taken within 15 ns of laser excitation indicate that the emission spectrum of the short-lived component is identical with that of the monomeric ruthenium complex. We have prepared the tetranuclear cluster in which all four metal centers are Ru, $\{[(bpy)_2Ru(L-L)]_3Ru\}$, with L–L being **3**.[18] The luminescence decay of this complex exhibits *no* short-lived component.

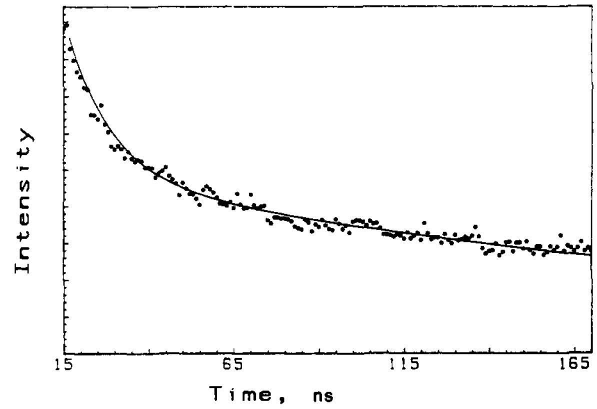

Figure 4. Room-temperature emission decay at 620 nm of a solution of **4a** (1 × 10^{-4} M) and Fe(II) (5 × 10^{-4} M). The smooth curve is the best fit of the data using a double-exponential fitting routing with a fixed lifetime for the long component of 360 ns.

Table III. Emission Spectral Characteristics of Complexes **1b–4b**[a]

complex	τ(298 K), ns	$\tau_{complex}$/ τ°_{free}(298 K)	$\phi_{complex}$/ ϕ°_{free}(298 K)[b]	τ(77 K), ns
1b	6 ± 2	0.017	0.10	45 ± 5
2b	52 ± 4	0.13	0.36	110 ± 10
3b	38 [illegible] 3	0.10	0.33	100 ± 10
4b	92 ± 8	0.26	0.31	85 ± 5

[a] Lifetimes determined for in situ mixtures of the free Ru(II) complex and the tetranuclear complex (see Experimental Section), assuming double-exponential decay. [b] Obtained from fits of $\phi_{complex}/\phi^{\circ}_{free}$ vs. [Fe(II)].

Lifetimes for the short-lived component, determined by fitting observed decays as double exponentials, are given in Table III. The lifetimes depend strongly on the length of the hydrocarbon link between the bipyridines at room temperature yet vary by only a factor of 2 at 77 K. Assuming the short-lived component corresponds to decay of the tetranuclear complexes (**1b–4b**), the limiting ratio of lifetimes $\tau_{complex}/\tau^{\circ}$ may be determined as listed in Table III. Included also are the limiting quantum yield ratios $\phi_{complex}/\phi^{\circ}_{free}$ determined from fits of emission intensity as a function of added Fe(II) (Figure 3). The fact that the $\tau_{complex}/\tau^{\circ}$ and $\phi_{complex}/\phi^{\circ}_{free}$ values are not the same for each complex suggests that complexes other than tetranuclear clusters exist in solution at high [Fe(II)] (vide infra). An observation relating to this discrepancy appears in the lifetime measurements. The fraction of the total emission arising from the short-lived component, determined from the magnitude of the prefactors for the two decay components, increases with added Fe(II) up to Fe:Ru ratios of 4. Further addition of Fe(II) results in a decrease in the fraction of the short-lived component, suggesting a decrease in the relative amount of the tetranuclear complex.

Discussion

Stoichiometry and Fast-Emission Decays. Iron bipyridyl and phenanthroline complexes have distinct MLCT transitions in the visible that allow them to be distinguished from ruthenium analogues.[15] The iron(II) → bipyridine MLCT characteristic of $[Fe(bpy)_3]^{2+}$ appears in the absorption spectra of complexes **1b**–**4b** after subtraction of the absorption of **1a**–**4a** (Figure 1b). Further evidence for formation of **1b**–**4b** is provided by spectrophotometric titrations (by Job's method) and cyclic voltammetry of the PF_6^- salt of the complex formed with **3a**.

The fast luminescence decays at 620 nm in solutions containing **1b**–**4b** result from intramolecular energy transfer from excited ruthenium(II) bipyridyl centers to the iron(II) bipyridyl at the center of the cluster. This assignment is based upon consideration of the following indirect evidence:

(1) Quenching of $[Ru(bpy)_3]^{2+}$ by both $Fe(II)_{aq}$[16] and $[Fe(bpy)_3]^{2+}$ [17] occurs with respective rates of 10^7 and 10^9 M^{-1} s^{-1}. At the concentrations of Fe(II) used in this work, quenching of $[Ru(bpy)_3]^{2+}$ by Fe(II) does not occur in 1:1 methanol:water.

(2) The quenching behavior mirrors the absorbance increase at 525 nm, which indicates formation of the tetranuclear cluster.

(3) The luminescence lifetime of $\{[(bpy)_2Ru(L\text{-}L)]_3Ru\}^{8+}$, where L-L is **3** is very similar to that of complex **3a**, and *no* short-lived component is observed with low intensity excitation.[18]

(4) The magnitude of the fast decay relative to the long-lived decay of **1a**–**4a** increases with increases in the Fe:Ru molar ratio (vide infra).

Energy-Transfer Mechanism. Electronic energy-transfer processes occur generally by one of two mechanisms: coupling of donor and acceptor transition multipoles[19] or electron exchange between the donor and acceptor.[20] The strongest multipole component for this process is dipole-coupling (Förster) transfer. Experimentally, Förster transfer differs from the electron-exchange mechanism in the distance dependence of the energy transfer rate. The energy transfer rate falls off as r^6 in the dipole-coupling mechanism whereas the electron-exchange transfer rate decreases exponentially with separation. The dipole-coupling mechanism also depends on the magnitude of the molar absorptivity of the acceptor absorption in the region of overlap of the donor emission and acceptor absorption.[19a] In the exchange mechanism, overlap is important only as a measure of the probability of system isoenergetics for exchange, thus electron exchange usually dominates for energy transfer between forbidden transitions.

Quenching of $[Ru(bpy)_3]^{2+}$ by $[Fe(bpy)_3]^{2+}$ in aqueous solution occurs with a rate constant of 10^9 M^{-1} s^{-1}. The acceptor transition for the energy transfer, as discussed by Sutin, very likely involves weak transitions of $[Fe(bpy)_3]^{2+}$ such as the $^1A \rightarrow {}^1T_1$, $^1A \rightarrow {}^3T_2$, or $^1A \rightarrow {}^1T_2$ ligand field transitions or the $^1A \rightarrow {}^3$MLCT transition.[17] Direct overlap of the intense $^1A \rightarrow {}^1$MLCT absorption of $[Fe(bpy)_3]^{2+}$ with the ruthenium emission is small, and, as a result, energy transfer in solution probably occurs via an electron-exchange mechanism. For complexes **1b**–**4b**, the donor and acceptor centers have metal center to metal center separations ranging from 10 Å (**1b**) to 17 Å (**4b**), assuming fully extended hydrocarbon chains. Distances of the hydrocarbon linkage between the bridging bipyridines on the donor and acceptor range from 1.5 to 9 Å. At such distances the dipole-coupling mechanism is feasible; the critical transfer distance at 298 K (where $k_{EN} = 1/\tau°$) for this system is 14 Å on the basis of Förster's theory of energy transfer (eq 2), where k_{EN} is the rate constant for energy transfer,

$$k_{EN} = 1.25 \times 10^{17}(\phi_E/n^4\tau_D r^6) \int_0^\infty F_D(\bar{\nu})\ \epsilon_A(\bar{\nu})\ d\bar{\nu}/\bar{\nu}_4 \quad (2)$$

ϕ_E is the donor emission quantum yield, n is the solvent refractive index, τ_D is the donor excited-state lifetime, r is the distance of separation of donor and acceptor, and the integral term represents the spectral overlap of the normalized donor emission with the acceptor absorption in the region of overlap. At separations less than the critical distance, energy transfer is faster than radiative and nonradiative relaxation of the donor. In fluid solution, long-range Förster transfer can be distinguished from exchange energy transfer if the observed emission quenching rate is faster than the diffusion-limited rate. Since complexes **1b**–**4b** all have donor–acceptor separations less than the critical transfer distance, dipolar coupling of the ruthenium emission with the iron $^1A \rightarrow {}^1$MLCT transition is possible.

Table IV. Rates of Intramolecular Energy Transfer for Complexes **1b**–**4b**

complex	10^6k_{EN}, s^{-1} 295 K	10^6k_{EN}, s^{-1} 77 K	R,[a] Å
1b	197 ± 65	22 ± 3	10
2b	17 ± 1	9 ± 1	11.5
3b	24 ± 2	10 ± 1	14
4b	8 ± 0.7	12 ± 1	17

[a] All distances ±1 Å determined from space-filling molecular models and represent the metal center to metal center distance. The dipole–dipole separation will be less than this distance.

Table IV lists k_{EN} for **1b**–**4b** determined from luminescence lifetime measurements[26] at 298 and 77 K as well as approximate dipole–dipole separations measured by using space-filling molecular models. Comparison of the measured k_{EN} values with the rate constant for homogeneous solution quenching of $[Ru(bpy)_3]^{2+}$ by $[Fe(bpy)_3]^{2+}$ can be accomplished by employing steady-state kinetic analysis of the solution quenching, assuming back-transfer from $[Fe(bpy)_3]^{2+*}$ to $[Ru(bpy)_3]^{2+}$ is unimportant (eq 3), where

$$\frac{1}{k_q} = \frac{1}{k_{diff}} + \frac{1}{k'_q} \quad (3a)$$

$$k'_q = k_{EN}K_{assoc} \quad (3b)$$

k_q is the observed quenching rate constant, k_{diff} is the diffusion-limited rate constant and K_{assoc} is the equilibrium constant for formation of the precursor complex to energy transfer.[21] K_{assoc} is estimated from the Eigen–Fuoss equation,[22] and k_{diff} is approximated by using the Debye–Smoluchouski[23] equation. If the literature value for k_q[17] and the above calculated constants are employed, k_{EN} is 2.5×10^9 s^{-1} at room temperature, a value greater than that observed for intramolecular quenching in **1b**–**4b**. Conformational restrictions imposed by the alkyl chain linking the donor and acceptor in **1b**–**4b** certainly influence the energy-transfer process. Conformational effects have been observed for energy transfer in organic donor–acceptor complexes[24] and very recently for intramolecular electron-transfer quenching in a covalently linked ruthenium bipyridyl–diquat system.[25] Thus, from the above comparison, the dipole–dipole and exchange-energy-transfer mechanisms cannot be distinguished.

In frozen solution (Table IV, 77 K data), k_{EN} varies by less than a factor of 3 among the four complexes, compared to a 25-fold variation at room temperature. A large decrease in k_{EN} is observed for **1b** while a small increase in k_{EN} is observed for **4b**. Since the series does not exhibit a systematic distance dependence for k_{EN} in frozen solution, it suggests that the Förster mechanism is not important. However, the low-temperature absorption of $[Fe(bpy)_3]^{2+}$ does overlap with the 77 K emission of **1a**–**4a** and a critical transfer distance of 19 ± 2 Å results. Thus, Förster transfer must occur for **1b**–**4b** in frozen solution. In fact, decay of **1b**–**3b** is slower than that predicted for Förster transfer alone. Only complex **4b** exhibits an energy transfer rate faster than predicted for Förster transfer at 77 K. As a result, the 77 K luminescence lifetime information does not allow ruling out contact energy transfer.

On the basis of the above observations, the definitive experiment with this system requires isolating **1b**–**4b**, separated from free complex **1a**–**4a**, and measuring both room temperature and 77 K lifetimes. All complexes should have only a single fast component at room temperature. In frozen solutions complex **4b** and possibly **2b** and **3b** will exhibit both fast and slow decay components since conformations should exist for these molecules that exhibit very little quenching if exchange-energy transfer predominates. Since the donor–acceptor separation is less than R_0 (19 Å), for **1b**–**4b**, the Förster mechanism predicts observable transfer for all conformations of **1b**–**4b** in frozen solution. Currently, isolation of **1b**–**4b** in the absence of **1a**–**4a** is not possible.

Steady-State Quenching vs. Transient Decay. As noted above, limiting values of $\phi_{complex}/\phi°_{free}$ at high Fe(II) concentrations are much larger than limiting values of $\tau_{complex}/\tau°_{free}$, and the short-lived transient decreases in intensity relative to the long-lived emission component upon increasing [Fe(II)]:[Ru(II)] above 4:1. Because experiments are performed by adding Fe(II) to solutions having a fixed concentration of complexes **1a–4a**, the dissociation of the product complex **1b–4b** to form $\{[(bpy)_2Ru(L\text{-}L)]_2Fe(S)_2\}$, where S is solvent, becomes important at high concentrations of iron(II). The resulting high-spin iron(II) complex should be a weaker quencher of excited ruthenium bipyridyl centers than the low-spin iron complexes **1b–4b**. For $[Fe(bpy)_3]^{2+}$ the analogous reaction, shown in eq 4, has an equilibrium constant of 10^{-8}.[13]

$$2[Fe(bpy)_3]^{2+} + [Fe(OH_2)_6]^{2+} \rightleftarrows 3[Fe(bpy)_2(OH_2)_2]^{2+} \quad (4)$$

However, for **1b–4b** the constant for this process should be much higher since there are significant steric and coulombic repulsion factors for the "ligands" **1a–4a**. The decrease in K_{eq} for formation of **1b–4b** with decreasing bridge length, R, supports a process similar to eq 4 as the mechanism for the decrease in quenching at high [Fe(II)]. Further, a decrease in the absorbance due to **1b–4b** at 525 nm is observed at high [Fe(II)]. As a result, the degree of emission quenching at high [Fe(II)] decreases and the limiting $\phi_{complex}/\phi^{\circ}_{free}$ (Figure 3) value does not reflect complete complexation of **1a–4a** to form **1b–4b**. Since $\tau_{complex}/\tau^{\circ}_{free}$, represents the limiting value for lifetimes, it is much smaller than $\phi_{complex}/\phi^{\circ}_{free}$ for each complex.

Conclusion

This work demonstrates that uncomplexed bipyridines covalently attached in tris(bipyridyl)ruthenium(II) derivatives can be effectively used as ligands for complexation to other metals to prepare polynuclear clusters having high charge. In situ preparation of the tris Fe(II) complexes **1b–4b** only partially quenches the ruthenium bipyridyl emission via energy transfer. Communication between the ruthenium bipyridyl donor and the iron bipyridyl acceptor depends on the length of the covalent linkage between the two centers.

Acknowledgment. Support by the National Science Foundation (Grant CHE-8214299) is gratefully acknowledged (C.M.E.). Acknowledgment is also made to the donors of the Petroleum Research Fund (R.H.S. and R.A.A.), administered by the American Chemical Society, for partial support of this work.

Contribution from the Guelph Waterloo Centre for Graduate Work in Chemistry, Guelph Campus,
Department of Chemistry and Biochemistry, University of Guelph, Guelph, Ontario N1G 2W1, Canada,
and Department of Chemistry, University of Arkansas, Fayetteville, Arkansas 72701

Redox Chemistry of 1,2,4,6-Thiatriazinyls: Preparation and Crystal Structures of 3,5-Diphenyl-1,2,4,6-thiatriazinium Hexafluorophosphate, $[Ph_2C_2N_3S]^+[PF_6]^-$, and 3,5-Diphenyl-4-hydro-1,2,4,6-thiatriazine, $[Ph_2C_2N_3SH]$

René T. Boeré,[1a] A. Wallace Cordes,[1b] Patrick J. Hayes,[1a] Richard T. Oakley,*[1a] Robert W. Reed,[1a] and William T. Pennington[1b]

Received December 5, 1985

The oxidation of 3,5-diphenyl-1,2,4,6-thiatriazinyl dimer with the nitrosonium salts $[NO]^+X^-$ ($X^- = BF_4^-, PF_6^-$) yields the corresponding salts of the $[Ph_2C_2N_3S]^+$ cation. Reduction of the same compound by sodium in liquid ammonia affords, following acidification, the reduced system 3,5-diphenyl-4-hydro-1,2,4,6-thiatriazine, $Ph_2C_2N_3SH$. The structures of $[Ph_2C_2N_3S]^+[PF_6]^-$ and $Ph_2C_2N_3SH\cdot0.5CH_2Cl_2$ have been determined by X-ray diffraction. The structural parameters of the triad of oxidation states of the C_2N_3S ring system, i.e. cation, radical dimer, and anion, are discussed in relation to the results of MNDO molecular orbital calculations on model compounds related to the three species. Crystals of $[Ph_2C_2N_3S]^+[PF_6]^-$ are monoclinic, space group $C2/c$, with $a = 18.170$ (4) Å, $b = 12.080$ (2) Å, $c = 7.748$ (3) Å, $\beta = 108.56$ (4)°, $V = 1612$ (2) Å^3, and $Z = 4$ at 22 °C and $R = 0.064$ for 1114 reflections with $I > 3\sigma(I)$. Crystals of $Ph_2C_2N_3SH\cdot0.5CH_2Cl_2$ are orthorhombic, space group $Pbcn$, with $a = 19.427$ (3) Å, $b = 9.900$ (2) Å, $c = 14.840$ (4) Å, $\beta = 90°$, $V = 2854$ (2) Å^3, and $Z = 8$ at 22 °C and $R = 0.047$ for 1152 reflections with $I > 3\sigma(I)$.

Introduction

The redox chemistry of binary sulfur nitride molecules and ions has been studied extensively. The electrochemical and chemical reduction of S_4N_4[2,3] leads via the radical anion $S_4N_4^-$[3] to the cyclic $S_3N_3^-$[4] ion, while its oxidation in strongly acidic media affords, inter alia, the dication $S_4N_4^{2+}$[5] and the radical $S_3N_2^+$[6] cation. A radical cation $S_4N_4^+$ has recently been postulated, but no spectroscopic evidence was provided.[7] Neutral radical systems are less common. Although the existence of the $S_3N_3^\bullet$ radical in the gas phase has been clearly demonstrated,[8] attempts to observe it in solution have been unsuccessful; both oxidation of $S_3N_3^-$ and reduction of $S_3N_3Cl_3$ yield S_4N_4.[2b,9] Because of this propensity of SN molecules and ions to undergo drastic structural rearrangements following electron transfer, their potential applications in the design of devices and electrocatalysts is limited.

One approach to remedying the structural instability of binary sulfur–nitrogen radicals is to modify them through incorporation of organic units. Several neutral organothiazyl radicals have now been characterized,[10–15] including the remarkably stable 3,5-di-

---

(1) (a) University of Guelph. (b) University of Arkansas.

(2) (a) Hojo, M. *Bull. Chem. Soc. Jpn.* **1980**, *53*, 2856. (b) Chivers, T.; Hojo, M. *Inorg. Chem.* **1984**, *23*, 1526. (c) Tweh, J. W.; Turner, A. G. *Inorg. Chim. Acta* **1981**, *48*, 173.

(3) (a) Brown, O. R. *J. Electroanal. Chem. Interfacial Electrochem.* **1972**, *34*, 419. (b) Williford, J. D.; Van Reet, R. E.; Eastman, M. P.; Prater, K. B. *J. Electrochem. Soc.* **1973**, *120*, 1498.

(4) Bojes, J.; Chivers, T.; Laidlaw, W. G.; Trsic, M. *J. Am. Chem. Soc.* **1979**, *101*, 4517.

(5) Gillespie, R. J.; Kent, J. P.; Sawyer, J. F.; Slim, D. R.; Tyrer, J. D. *Inorg. Chem.* **1981**, *20*, 3799.

(6) (a) Gillespie, R. J.; Kent, J. P.; Sawyer, J. F. *Inorg. Chem.* **1981**, *20*, 4053. (b) Roesky, H. W.; Hamza, A. *Angew. Chem., Int. Ed. Engl.* **1976**, *15*, 226. (c) Krebs, B.; Henkel, G.; Pohl, S.; Roesky, H. W. *Chem. Ber.* **1980**, *113*, 226.

(7) Muller, U.; Conradi, E.; Emart, U.; Dehnicke, K. *Angew. Chem., Int. Ed. Engl.* **1984**, *23*, 237.

(8) (a) Lau, W. M.; Westwood, N. P. C.; Palmer, M. C. *J. Chem. Soc., Chem. Commun.* **1985**, 752. (b) Lau, W. M.; Westwood, N. P. C.; Palmer, M. C. *J. Am. Chem. Soc.*, in press.

(9) Oakley, R. T., unpublished results.

(10) Wolmershäuser, G.; Schnauber, M.; Wilhelm, T. *J. Chem. Soc., Chem. Commun.* **1984**, 573.

(11) (a) Fairhust, S. A.; Pilkington, R. S.; Sutcliffe, L. H. *J. Chem. Soc., Faraday Trans. 1* **1983**, *79*, 439, 925. (b) MacLean, G. K.; Passmore, J.; Schriver, M. J.; White, P. S.; Bethell, D.; Pilkington, R. S.; Sutcliffe, L. H. *J. Chem. Soc., Chem. Commun.* **1983**, 807.

(12) Kaplan, M. L; Haddon, R. C.; Hirani, A. M.; Schilling, F. C.; Marshall, J. H. *J. Org. Chem.* **1981**, *46*, 675.

(13) Banister, A. J.; Smith, N. R. M.; Hey, R. G. *J. Chem. Soc., Perkin Trans 1* **1983**, 1181.

0020-1669/86/1325-2445$01.50/0 © 1986 American Chemical Society